mathematics

MDPI

Article

On the Necessary Conditions for Non-Equivalent Solutions of the Rotlet-Induced Stokes Flow in a Sphere: Towards a Minimal Model for Fluid Flow in the Kupffer's Vesicle

Yunay Hernández-Pereira [1], Adán O. Guerrero [2], Juan Manuel Rendón-Mancha [1] and Idan Tuval [3,*]

[1] Centro de Investigación en Ciencias, Instituto de Investigación en Ciencias Básicas y Aplicadas, Universidad Autónoma del Estado de Morelos, Av. Universidad 1001, Chamilpa, Cuernavaca 62209, Morelos, Mexico; yunayh@gmail.com (Y.H.-P.); rendon@uaem.mx (J.M.R.-M.)

[2] Laboratorio Nacional de Microscopía Avanzada, Instituto de Biotecnología, Universidad Nacional Autónoma de México, Mexico City 62210, Mexico; adanog@ibt.unam.mx

[3] Mediterranean Institute for Advanced Studies (CSIC-UIB), 07190 Esporles, Balearic Islands, Spain

* Correspondence: ituval@imedea.uib-csic.es

Received: 14 November 2019; Accepted: 16 December 2019; Published: 18 December 2019

Abstract: The emergence of left–right (LR) asymmetry in vertebrates is a prime example of a highly conserved fundamental process in developmental biology. Details of how symmetry breaking is established in different organisms are, however, still not fully understood. In the zebrafish (*Danio rerio*), it is known that a cilia-mediated vortical flow exists within its LR organizer, the so-called Kupffer's vesicle (KV), and that it is directly involved in early LR determination. However, the flow exhibits spatio-temporal complexity; moreover, its conversion to asymmetric development has proved difficult to resolve despite a number of recent experimental advances and numerical efforts. In this paper, we provide further theoretical insight into the essence of flow generation by putting together a minimal biophysical model which reduces to a set of singular solutions satisfying the imposed boundary conditions; one that is informed by our current understanding of the fluid flow in the KV, that satisfies the requirements for left–right symmetry breaking, but which is also amenable to extensive parametric analysis. Our work is a step forward in this direction. By finding the general conditions for the solution to the fluid mechanics of a singular rotlet within a rigid sphere, we have enlarged the set of available solutions in a way that can be easily extended to more complex configurations. These general conditions define a suitable set for which to apply the superposition principle to the linear Stokes problem and, hence, by which to construct a continuous set of solutions that correspond to spherically constrained vortical flows generated by arbitrarily displaced infinitesimal rotations around any three-dimensional axis.

Keywords: left–right asymmetry in vertebrates; Kupffer's vesicle; rotlet-induced internal Stokes flow

1. Introduction

In the early stages of development of the corporal patterns in multicellular organisms, cells become spatially arranged following a concrete body plan [1]. This process involves the laying down of the three decisive body axes: the anterior–posterior, dorsal–ventral and left–right axes, as seen in Figure 1A [2,3]. Although in most vertebrates, including humans, the external appearance is nearly left–right symmetric, our internal body arrangement is coordinated in a highly asymmetric fashion. In the most common disposition, known as *situs solitus*, the heart is on the left and the liver on the

right side of the body. This orderly development and, most importantly, the many causes of its failure, have been the subject of extensive research with common fatal and benign pathologies [4,5] being associated with the abnormal (i.e., heterotaxy), random (*situs ambiguus*) or mirror-reversed (*situs inversus*) arrangement of internal organs.

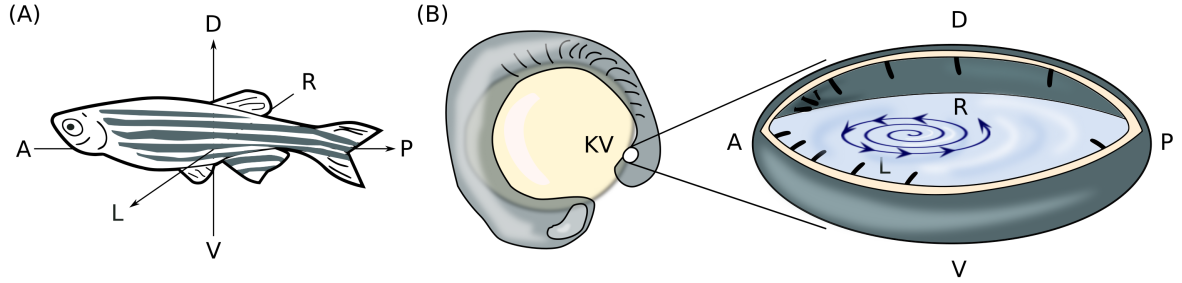

Figure 1. The flow field within the Kupffer's vesicle (KV) determines the left–right axis. (**A**) The corporal axes of the zebrafish: anterior–posterior (A,P), dorso–ventral (D,V) and Left–Right (L,R). (**B**) Location of the organizer in the zebrafish embryo, and the cilia driven vortical flow within the KV.

In many organisms, left–right symmetry breaking occurs within a specialized group of cells forming a transient organ generically referred to as the "organizer" [2,3]. Elegant experimental and theoretical work has established the role of physics and, in particular, of fluid dynamics in this process. By using mice as a model system, this was first demonstrated by Nonaka et al. in 2002 in what has become a seminal work in the field [6]: In the node, tens of incessantly circling monocilia, tilted toward the posterior axis [7], collectively generate a leftward flow that effectively breaks the left–right symmetric development. The flow is understood to either serve as the carrier of a chemical morphogenic signal or to act as an intrinsic mechanical signal for the subsequent cascade of genetic and developmental events [3,8]. The nodal flow hypothesis is still to date one of the most exquisite examples of the constructive role of fluid mechanics in establishing fundamental patterns in early vertebrate development [6,9–12].

In the zebrafish *Danio rerio*, one of the best studied model organisms for vertebrate development, the corresponding left–right organizer (i.e., the Kupffer's vesicle (KV)) has, similarly to mice, one layer of monociliated epithelial cells that line a lumen cavity filled with extracellular fluid [13] (see Figure 1B). Once again, the minute forces generated by tens of motile monocilia are enough to set in motion a KV flow [14]. However, accurately pinpointing the left–right asymmetric features of the flow has proved more difficult. Firstly, this is because the three-dimensional geometry of the KV cavity, compared to the effectively two-dimensional nodal case, leads to more complex three-dimensional fluid flow patterns [15]. Secondly, it is also because the flow exhibits spatiotemporal complexity [16]. The experimental observation of the existence of a relatively simple counter-clockwise circulation (when seen from the dorsal side) in the coronal mid-plane of the KV [17], as depicted in Figure 1B (right), is not enough to clarify the development of laterality. Such flow would remain left–right symmetric unless cilia orientation, spatial distribution or beating characteristics dictate otherwise. Despite recent progress in the modelling and experimental description of cilia beating and fluid flow within the KV [18,19], these details are not yet completely resolved.

From the modelling perspective, progress in the field has been facilitated by the use of exact and approximate analytical and numerical methods with which to tackle Stokes equations for the fluid mechanics of incompressible viscous flows. The Stokes regime is a simplification of the Navier–Stokes equations for when the inertial effects are negligible compared to viscous forces; i.e., it is a valid approximation for the very low-Reynolds-number regime typically encountered at the micro scale [20]. Research in polymer science and suspension rheology, micro-organism locomotion and other biophysical flows or large scale, but slow, geophysical flows, have all been based in one way or another in the Stokes equation. At the same time, these distinct scientific disciplines have all largely contributed to the development of appropriate mathematical methods with which to tackle its analysis.

Nevertheless, finding exact solutions for arbitrary boundary conditions are still recognized as a difficult task with only a limited number of closed-form solutions known to date and only for the simplest highly symmetric geometric configurations [21].

A powerful analytical method available for finding approximate solutions to Stokes flows is the so called 'singularity method' (SM). Pioneered by Lorentz, Oseen and Burgers [22–24], it is based on a multipole expansion of the exact solution for a singular (i.e., delta-like in space) forcing term in the equation. By choosing the appropriate spatial distribution of individual terms from the expansion (i.e., the basic singularities known as Stokeslet, Rotlet (also called a Couplet by Batchelor [25]), Stresslet and others), it is possible to address complex steady and time-dependent problems. Examples abound and they include the use of SM for studies of slender-body, boundary element or mesh free methods in disparate branches of fluid mechanics [25–36].

SM has been already successfully employed to construct physical descriptions of the fluid mechanics of the fluid flow within the left–right (LR) organizers (both in the case of the mouse Hensen's node and in the zebrafish KV) and to express, analyse and predict through mathematical and computational models the characteristics of these fluid flows [7,14,15,18]. Following a similar modelling spirit, we set here to seek for a closed-form solution to the KV flow, aiming to provide theoretical insight into the essence of flow generation by the use of conceptually simplified physics models. Specifically, we reduce the flow to a sum of rotational solutions but, instead of modelling the flow induced by each individual circling cilia as previously done in [7] for the mouse node and in [19] for the KV, we consider a single rotational singularity to account for the overall vortical structure of the KV flow. Moreover, we elucidate the required geometric constraints necessary to obtain a set of non equivalent solutions for the rotlet-induced internal Stokes flow within a simplified rigid spherical geometry. While the literature already provides one such an exact solution to the same problem [36], this is restricted to a very specific geometric configuration of the three-dimensional rotlet: Radially displaced along one of the axis of the sphere (e.g., the z-axis) while pointing orthogonally to it (e.g., parallel to the y-axis). Here, instead, we address the general conditions for existence of other independent solutions compatible with the symmetry and boundary conditions of the problem. By doing so, we will be able to address possible LR asymmetries in the established fluid flows that arise from anterior–posterior and dorsal–ventral asymmetries in the force field.

2. Results

2.1. Definition of the Problem and Preliminaries

The zebrafish KV is a roughly spheroidal structure approximately $70 \times 60 \times 30\ \mu m^3$ in size, transiently located at the tip of the developing embryo during early somitogenesis, Figure 1B. It is filled with fluid set in motion by tens of 2–4 μm long cilia lining its inner cell layer [15]. These beating cilia generate a predominantly vortical anticlockwise fluid flow when viewed from the dorsal side, with a centre shifted towards the anterior end [17]. The small scale of the KV together with the slow speed of the KV flow imply that, from a fluid mechanics perspective, we are well within the realm of low Reynolds number flows, with $Re \lesssim 10^{-3}$ [15]. In the context just described, the correct fluid mechanics within the KV is simply modelled by the Stokes equations for an incompressible fluid together with conditions for the boundary problem, namely:

$$\begin{aligned} \nabla p - \mu \nabla^2 u &= f \\ \nabla \cdot u &= 0 \\ u|_{\partial\Omega} &= 0 \\ \Omega &: sphere. \end{aligned} \tag{1}$$

Here $p = p(x)$ and $u = u(x)$ are the pressure and fluid velocity field at position x respectively, μ is the fluid viscosity, f the resultant of the body forces responsible for the fluid motion and $x \in \Re^3$.

Moreover, the fluid is subjected to the usual no-slip (Dirichlet) boundary conditions with the flow velocity approaching zero close to the surface cell layer, an expected and experimentally confirmed fact in the KV [14–16,19]. A convenient representation in spherical coordinates of the general solution to the system of Equation (1) was given by Ranger [37] in the form:

$$\begin{aligned} u(r,\theta,\phi) &= curl^2\left[\frac{\vec{r}\psi(r,\theta)}{r\ sin\theta}cos\phi\right] + curl\left[\frac{\vec{r}\chi(r,\theta)}{r\ sin\theta}sin\phi\right] \\ p(r,\theta,\phi) &= \frac{\mu}{r\ sin\theta}\frac{\partial}{\partial r}\left[\frac{\partial^2\psi(r,\theta)}{\partial r^2} + \frac{sin\theta}{r^2}\frac{\partial}{\partial\theta}\left(\frac{1}{sin\theta}\frac{\partial\psi(r,\theta)}{\partial\theta}\right)\right]cos\phi \end{aligned} \tag{2}$$

where the spherical coordinates (r,θ,ϕ) are related to the Cartesian position vector x in the usual way, $r\in[0,1]$, $\theta\in[0,\pi]$ and $\phi\in[0,2\pi)$, and the scalar functions ψ and χ satisfy:

$$L_{-1}^2\psi = L_{-1}\chi = 0 \tag{3}$$

with the Stokes operator L_{-1} defined by $L_{-1}\equiv\frac{\partial^2}{\partial r^2}+\frac{sin\theta}{r^2}\frac{\partial}{\partial\theta}\left(\frac{1}{sin\theta}\frac{\partial}{\partial\theta}\right)$ or, expressing the velocity field in its spherical components,

$$\begin{aligned} u_r(r,\theta,\phi) &= -\frac{1}{r^2}\frac{\partial}{\partial\theta}\left[\frac{1}{\sin\theta}\frac{\partial\psi}{\partial\theta}\right]\cos\phi \\ u_\theta(r,\theta,\phi) &= \left[\frac{1}{r}\frac{\partial}{\partial\theta}\left(\frac{1}{\sin\theta}\frac{\partial\psi}{\partial r}\right) + \frac{\chi}{r\ \sin^2\theta}\right]\cos\phi \\ u_\phi(r,\theta,\phi) &= -\left[\frac{1}{r\ \sin^2\theta}\frac{\partial\ \psi}{\partial r} + \frac{1}{r}\frac{\partial}{\partial\theta}\left(\frac{\chi}{\sin\theta}\right)\right]\sin\phi. \end{aligned} \tag{4}$$

As described above, the KV flow is known to be predominantly vortical, viscous, incompressible, approximately Newtonian and non-axisymmetric [14,15,18]. In order to construct a minimal model for the KV fluid flow capturing all these experimentally observed features, we decided to focus on the simplest singular solution capable of providing vortical fluid motion with the correct approximate geometry: a single rotlet embedded within a rigid spherical shell filled with a viscous and incompressible fluid (Figure 2A). This is, in principle, also a solution that is amenable to extensive parametric analysis and that can be easily extended to more complex configurations. It is important to notice, however, that, in contrast to previous work [7,15,18,19], here we are not using a rotlet (or any other singular solutions) to model the flow around individual beating cilia but rather to describe the overall vortical structure that emerges in the KV from tens of cilia simultaneously pumping the fluid.

More specifically, we consider a rotlet of torque $\mathbf{L} = (l_1, l_2, l_3)$ (with $l_1, l_2, l_3 \in \Re$), centred at position $\mathbf{x_0} = (x_0, y_0, z_0)$ (or (c, θ_0, ϕ_0) in spherical coordinates) within the unit sphere, with the origin of our coordinate system, O, fixed at its centre as depicted in Figure 2A. We first recall that in an unbounded three dimensional space, the solution u_0 to the Stokes problem defined above with the flow decaying to zero at infinity, takes the simplified form:

$$u_0 = \frac{\mathbf{L}\times\mathbf{R}}{8\pi\left\|R\right\|^3} \tag{5}$$

which can be interpreted as the flow induced by the rotation of an infinitesimally small sphere in a viscous fluid [38,39], and it corresponds to the first axisymmetric term in the multi-pole expansion solution to Equation (1). Here $\mathbf{R}$ is the relative position vector $\mathbf{R}\equiv\mathbf{x}-\mathbf{x_0}$, and $\|R\|$ its l^2-norm.

For an unbounded flow there is always a simple geometric transformation, consisting in a three-dimensional rotation plus translation, that brings $\mathbf{x_0}$ to O, and $\mathbf{L}$ to $\hat{k}$. However, with the boundary conditions on the sphere defined in Equation (1), the solution to the boundary problem becomes uniquely dependent on the position and orientation of the torque vector $\mathbf{L}$. Hackborn et al. [36] obtained a particular solution to this problem restricted to a very specific geometric configuration of

the three-dimensional rotlet: radially displaced along one the z-axis, i.e., $\mathbf{x_0} = (0, 0, c)$, while pointing parallel to the y-axis, i.e., $\mathbf{L} = (0, 1, 0)$. Moreover, they provided a convenient closed-form for the scalar functions ψ and χ. Figure 2C,D show a few streamlines computed from this solution for $c = 0.25$ and a set of random initial conditions on the $z = 0$ plane. Figure 2B further compares the flow within a rigid sphere to the unbounded. As can be seen there, the major difference arises close to the $r = 1$ boundary where the unbounded rotlet does not satisfy the required no-slip condition. In the next sections, we expand Hackborn's analysis to provide necessary geometric conditions for the existence of other independent solutions compatible with the symmetry and boundary conditions of the problem.

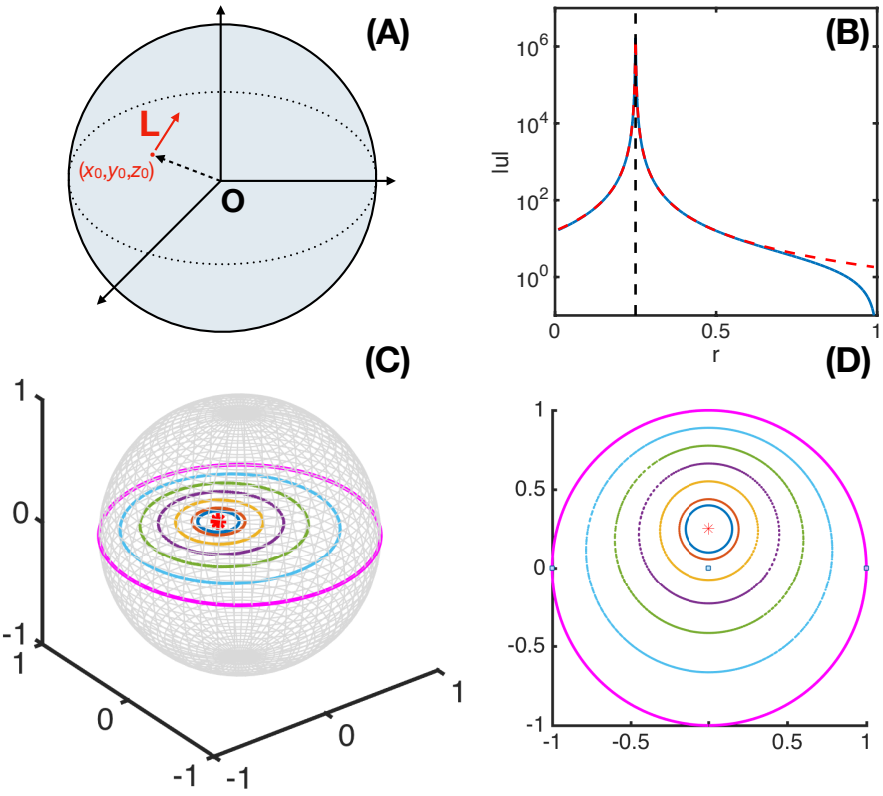

Figure 2. Rotlet in a sphere. (**A**) Definition of the system of reference, position and orientation of the rotlet. (**B**) A cross section of $\|u(r)\|$ comparing the bounded (Hackborn) and unbounded (rotlet) solutions. (**C**) 3D flow streamlines for Hackborn's solution, i.e., $(x_0, y_0, z_0) = (0, 0, c)$ and $\mathbf{L} = (0, 1, 0)$, with c = 0.25 and 7 randomly selected initial conditions on the coronal mid-plane. (**D**) Projection of the same streamlines in (C) into the XY plane clearly showing the vortical structure.

2.2. Necessary Conditions of a Three-Dimensional Rotlet with Spherically-Symmetric Boundary Conditions

We can start by focusing on the numerator of Equation (5) for the unbounded solution. The cross product defines the three Cartesian components of this reduced velocity field, u_0^*, as

$$u_0^* \equiv \mathbf{L} \times \mathbf{R} = \begin{vmatrix} \vec{i} & \vec{j} & \vec{k} \\ l_1 & l_2 & l_3 \\ x - x_0 & y - y_0 & z - z_0 \end{vmatrix} = (l_2 (z - z_0) - l_3 (y - y_0)) \vec{i} + (l_3 (x - x_0) - l_1 (z - z_0)) \vec{j} + (l_1 (y - y_0) - l_2 (x - x_0)) \vec{k} \quad (6)$$

which, after making the transformation to spherical coordinates, read:

$$\begin{pmatrix} u^*_{0r} \\ u^*_{0\theta} \\ u^*_{0\phi} \end{pmatrix} = \begin{pmatrix} \sin\theta\cos\phi & \sin\theta\sin\phi & \cos\theta \\ \cos\theta\cos\phi & \cos\theta\sin\phi & -\sin\theta \\ -\sin\phi & \cos\phi & 0 \end{pmatrix} \begin{pmatrix} u^*_{0x} \\ u^*_{0y} \\ u^*_{0z} \end{pmatrix} \tag{7}$$
$$= \begin{pmatrix} \sin\theta\cos\phi & \sin\theta\sin\phi & \cos\theta \\ \cos\theta\cos\phi & \cos\theta\sin\phi & -\sin\theta \\ -\sin\phi & \cos\phi & 0 \end{pmatrix} \begin{pmatrix} l_2(z-z_0) - l_3(y-y_0) \\ l_3(x-x_0) - l_1(z-z_0) \\ l_1(y-y_0) - l_2(x-x_0) \end{pmatrix}$$

or, recalling that $x_0 = c\sin\theta_0\cos\phi_0$, $y_0 = c\sin\theta_0\sin\phi_0$, $z_0 = c\cos\theta_0$ and rearranging by spherical components:

$$\begin{aligned} u^*_{0r} &= [l_2(r\cos\theta - z_0) - l_3(r\sin\theta\sin\phi - y_0)]\sin\theta\cos\phi \\ &\quad + [l_3(r\sin\theta\cos\phi - x_0) - l_1(r\cos\theta - z_0)]\sin\theta\sin\phi \\ &\quad + [l_1(r\sin\theta\sin\phi - y_0) - l_2(r\sin\theta\cos\phi - x_0)]\cos\theta \\ &= [l_3y_0 - l_2z_0]\sin\theta\cos\phi + [l_1z_0 - l_3x_0]\sin\theta\sin\phi + [l_2x_0 - l_1y_0]\cos\theta \\ u^*_{0\theta} &= [l_2(r\cos\theta - z_0) - l_3(r\sin\theta\sin\phi - y_0)]\cos\theta\cos\phi \\ &\quad + [l_3(r\sin\theta\cos\phi - x_0) - l_1(r\cos\theta - z_0)]\cos\theta\sin\phi \\ &\quad - [l_1(r\sin\theta\sin\phi - y_0) - l_2(r\sin\theta\cos\phi - x_0)]\sin\theta \\ &= [l_2r - l_2z_0cos\theta + l_3y_0\cos\theta]\cos\phi + [l_1z_0cos\theta - l_3x_0cos\theta - l_1r]\sin\phi \\ &\quad + [l_1y_0 - l_2x_0]\sin\theta \\ u^*_{0\phi} &= -[l_2(r\cos\theta - z_0) - l_3(r\sin\theta\sin\phi - y_0)]\sin\phi \\ &\quad + [l_3(r\sin\theta\cos\phi - x_0) - l_1(r\cos\theta - z_0)]\cos\phi \\ &= [l_2z_0 - l_2r\cos\theta - l_3y_0]\sin\phi + l_3r\sin\theta + [l_1z_0 - l_1r\cos\theta - l_3x_0]\cos\phi. \end{aligned} \tag{8}$$

For the spherically-symmetric boundary conditions to be satisfied, the convenient representation in spherical coordinates given in Equation (4) further constraints the reduced velocity to the form $u^*_0 = \left(u'_{0r}\cos\phi, u'_{0\theta}\cos\phi, u'_{0\phi}\sin\phi\right)$ [37]. Here $u'_0 = (u'_{0r}, u'_{0\theta}, u'_{0\phi})$ should in general be considered a function of the three spherical coordinates $u'_0(r,\theta,\phi)$. However, it is sometimes convenient to reduce the problem even further by only looking for solutions for which $u'_0(r,\theta)$ is independent of ϕ, as it is the case in the particular solution obtained in [36]. These two complementary approaches will be discussed in the next two sections.

2.3. On Some General Conditions

It immediately follows from Equation (8) that u'_0 must satisfy:

$$\begin{aligned} u'_{0r} &= (l_3y_0 - l_2z_0)\sin\theta + (l_1z_0 - l_3x_0)\sin\theta\tan\phi + \frac{(l_2x_0 - l_1y_0)\cos\theta}{\cos\phi} \\ u'_{0\theta} &= l_2r + (l_3y_0 - l_2z_0)\cos\theta + (l_1z_0\cos\theta - l_3x_0\cos\theta - l_1r)\tan\phi + \frac{(l_1y_0 - l_2x_0)\sin\theta}{\cos\phi} \\ u'_{0\phi} &= (l_2z_0 - l_3y_0) - l_2r\cos\theta + (l_1z_0 - l_1r\cos\theta - l_3x_0)\cot\phi + \frac{l_3r\sin\theta}{\sin\phi} \end{aligned} \tag{9}$$

where, for the above to be valid, $\sin\phi \neq 0 \ \wedge \ \cos\phi \neq 0$. By using the representation of u given by Equation (4), we arrive at the following general necessary conditions for the corresponding potential functions ψ_0 and χ_0:

$$\begin{aligned}
-\frac{1}{r^2}\frac{\partial}{\partial\theta}\left[\frac{1}{\sin\theta}\frac{\partial\psi_0}{\partial\theta}\right] &= \frac{1}{R^3}\Big((l_3y_0 - l_2z_0)\sin\theta \\
&\quad + (l_1z_0 - l_3x_0)\sin\theta\tan\phi + \frac{(l_2x_0 - l_1y_0)\cos\theta}{\cos\phi}\Big), \\
\frac{1}{r}\frac{\partial}{\partial\theta}\left(\frac{1}{\sin\theta}\frac{\partial\psi_0}{\partial r}\right) + \frac{\chi_0}{r\sin^2\theta} &= \frac{1}{R^3}\Big(l_2r + (l_3y_0 - l_2z_0)\cos\theta \\
&\quad + (l_1z_0\cos\theta - l_3x_0\cos\theta - l_1r)\tan\phi + \frac{(l_1y_0 - l_2x_0)\sin\theta}{\cos\phi}\Big), \\
-\frac{1}{r\sin^2\theta}\frac{\partial\psi_0}{\partial r} - \frac{1}{r}\frac{\partial}{\partial\theta}\left(\frac{\chi_0}{\sin\theta}\right) &= \frac{1}{R^3}\Big(l_2z_0 - l_2r\cos\theta - l_3y_0 \\
&\quad + \frac{l_3r\sin\theta}{\sin\phi} + (l_1z_0 - l_1r\cos\theta - l_3x_0)\cot\phi\Big).
\end{aligned} \tag{10}$$

2.4. On Some Restricted Conditions

We next restrict our analysis to the simpler case where $u_0'(r,\theta)$ is independent of ϕ, for which the system of equations in Equation (8) reduces to:

$$\begin{aligned}
u^*_{0r} &= [l_3y_0 - l_2z_0]\sin\theta\cos\phi \\
u^*_{0\theta} &= [l_2r - l_2z_o\cos\theta + l_3y_0\cos\theta]\cos\phi \\
u^*_{0\phi} &= [l_2z_0 - l_2r\cos\theta - l_3y_0]\sin\phi
\end{aligned} \tag{11}$$

together with the following conditions:

$$\begin{aligned}
&\text{from } u^*_{0r}\text{:} \quad [[l_1z_0 - l_3x_0]\sin\theta\sin\phi + [l_2x_0 - l_1y_0]\cos\theta = 0] \\
&\vee [l_1z_0 - l_3x_0 = 0 \wedge l_2x_0 - l_1y_0 = 0]\,, \qquad (12) \\
&\text{from } u^*_{0\theta}\text{:} \quad [[l_1z_0\cos\theta - l_3x_0\cos\theta - l_1r]\sin\phi + [l_1y_0 - l_2x_0]\sin\theta = 0] \\
&\vee [l_1z_0\cos\theta - l_3x_0\cos\theta - l_1r = 0 \wedge l_1y_0 - l_2x_0 = 0]\,, \qquad (13) \\
&\text{from } u^*_{0\phi}\text{:} \quad [l_3r\sin\theta + [l_1z_0 - l_1r\cos\theta - l_3x_0]\cos\phi = 0] \\
&\vee [l_3 = 0 \wedge l_1z_0 - l_1r\cos\theta - l_3x_0 = 0]\,. \qquad (14)
\end{aligned}$$

The first condition in Equations (12)–(14) for each of the coordinates of the vector field leads to the system of equations:

$$\begin{aligned}
[l_1z_0 - l_3x_0]\sin\theta\sin\phi + [l_2x_0 - l_1y_0]\cos\theta &= 0 \\
[l_1z_0 cos\theta - l_3x_0\cos\theta - l_1r]\sin\phi + [l_1y_0 - l_2x_0]\sin\theta &= 0 \\
l_3r\sin\theta + [l_1z_0 - l_1r\cos\theta - l_3x_0]\cos\phi &= 0.
\end{aligned} \tag{15}$$

As (l_1, l_2, l_3) and (x_0, y_0, z_0) can all, in principle, be considered unknown variables (i.e., the system is compatible but has infinite solutions). Without any loss of generality, we can rearrange the system in Equation (15) by assuming (x_0, y_0, z_0) are dependent on (l_1, l_2, l_3). Finally, we solve for the independent variables by Gaussian reduction:

$$\begin{array}{c} \\ \sin\theta \\ \cos\theta \end{array} \begin{array}{c} \begin{array}{ccc} y_0 & z_0 & x_0 \end{array} \\ \left(\begin{array}{ccc|c} -l_1\cos\theta & l_1\sin\theta\sin\phi & l_2\cos\theta - l_3\sin\theta\sin\phi & 0 \\ l_1\sin\theta & l_1\cos\theta\sin\phi & -l_2\sin\theta - l_3\cos\theta\sin\phi & l_1 r\sin\phi \\ 0 & l_1\cos\phi & -l_3\cos\phi & l_1 r\cos\theta\cos\phi - l_3 r\sin\theta \end{array}\right) \end{array}$$

$$\sim \begin{array}{c} \begin{array}{ccc} y_0 & z_0 & x_0 \end{array} \\ \left(\begin{array}{ccc|c} -l_1\cos\theta & l_1\sin\theta\sin\phi & l_2\cos\theta - l_3\sin\theta\sin\phi & 0 \\ 0 & l_1\sin\phi & -l_3\sin\phi & l_1 r\cos\theta\sin\phi \\ 0 & 0 & 0 & l_3 r\sin\theta\sin\phi \end{array}\right) \end{array} \tag{16}$$

There is a solution for ($l_{1,2} \neq 0, l_3 = 0$) with the following dependent variables:

$$\begin{cases} x_0 = l_1(y_0 - r\sin\theta\sin\phi)/l_2 \\ y_0 \neq 0 \\ z_0 = r\cos\theta. \end{cases}$$

Taking into account that (x_0, y_0, z_0) have to take fix values in order to correspond to the position vector for the rotlet and, hence, that they can not depend on the spatial coordinates (r, θ, ϕ), the obtained result is not a physically meaningful solution for the problem at hand. On the contrary, the second set of conditions in Equations (12)–(14) specify that:

- If the condition in Equation (14) is met, we have

$$\begin{aligned} \text{if } l_3 = 0 \ &\rightarrow l_1 z_0 - l_1 r\cos\theta - l_3 x_0 = 0 \\ &\quad l_1\left(z_0 - r\cos\theta\right) = 0 \\ &\quad l_1 = 0 \vee z_0 = r\cos\theta. \end{aligned} \tag{17}$$

- If the conditions in Equations (13) and (17) are now both simultaneously satisfied then

$$\begin{aligned} \text{if } l_3 = 0 \ &\rightarrow l_1 z_0 - l_3 x_0 = 0 \wedge l_2 x_0 - l_1 y_0 = 0 \\ &\quad \underbrace{l_1 z_0 = 0}_{l_1 = 0 \vee z_0 = 0} \wedge l_2 x_0 = l_1 y_0 \\ &\quad \therefore l_1 = 0 \wedge \underbrace{l_2 x_0 = 0}_{l_2 = 0 \vee x_0 = 0} \\ &\quad \therefore x_0 = 0, \ \text{ because } \ l_2 \neq 0, \ \text{ given that } \ l_1 = l_3 = 0. \end{aligned} \tag{18}$$

This provides us with a suitable set of conditions for a general solution to Equation (4), namely, that the position and torque vectors for the rotlet take the form $\mathbf{x_0} = (0, y_0, z_0)$ and $\mathbf{L} = (0, l_2, 0)$. In the particular case of $y_0 = 0$ (and renaming $z_0 = c$) we recover the solution provided in [36] which describes the flow induced by a rotlet displaced along the z-axis and parallel to $\hat{y}$. For any other $y_0 \neq 0$, we arrive to a non-equivalent (independent) solution for which Equation (11) reduces to:

$$\begin{aligned} u^*_{0r} &= -l_2 z_0 \sin\theta\cos\phi \\ u^*_{0\theta} &= l_2\left(r - z_0 cos\theta\right)\cos\phi \\ u^*_{0\phi} &= l_2\left(z_0 - r\cos\theta\right)\sin\phi. \end{aligned} \tag{19}$$

Finally, and within this approach, the necessary conditions for the corresponding potential functions ψ_0 and χ_0 read:

$$\begin{aligned} -\frac{1}{r^2}\frac{\partial}{\partial\theta}\left[\frac{1}{\sin\theta}\frac{\partial\psi_0}{\partial\theta}\right] &= \frac{-l_2}{R^3}c\cos\theta_0\sin\theta, \\ \left[\frac{1}{r}\frac{\partial}{\partial\theta}\left(\frac{1}{\sin\theta}\frac{\partial\psi_0}{\partial r}\right)+\frac{\chi_0}{r\sin^2\theta}\right] &= \frac{l_2}{R^3}\left(r-c\cos\theta_0 cos\theta\right), \\ -\left[\frac{1}{r\sin^2\theta}\frac{\partial\psi_0}{\partial r}+\frac{1}{r}\frac{\partial}{\partial\theta}\left(\frac{\chi_0}{\sin\theta}\right)\right] &= \frac{l_2}{R^3}\left(c\cos\theta_0-r\cos\theta\right). \end{aligned} \tag{20}$$

We recall that within the spherical symmetry of the defined domain: (i) any arbitrary displacement from the origin can be assigned to a displacement along the z-axis by simple 3D rotations; (ii) any 3D orientation of the rotlet torque, L, can be assigned to an in-plane 2D (yz-plane) orientation by an appropriate rotation around the newly established z-axis; and (iii) any in-plane 2D (yz-plane) orientation can be decomposed in a component parallel and a component perpendicular to the y-axis. In this sense, and together with the solution provided in [26], these general conditions define a suitable set for which to apply the superposition principle to the linear Stokes problem Equation (1) and, hence, by which to construct a continuous set of solutions that correspond to spherically constrained vortical flows generated by arbitrarily displaced infinitesimal rotations around any three-dimensional axis.

3. Conclusions

Fluids shape ontogeny [40]. Biology makes use of the physics at hand to transduce signals into forces, and forces into shapes. And in nearly all cases, fluids (and fluid motion) are involved, either being the carriers of the transduced signals, the force actuators or sometimes even playing a dual role. Examples abound: from planar cell polarity (PCP) [41] to cytoplasmic streaming [42]; from lumen fracking establishing the AP axis [43], to the nodal flow in developing vertebrates [7], and many other cases of internal and external flows.

Having the correct set of theoretical tools to address the mathematical modelling of such instances is essential. However, analytical solutions to the equations describing fluid motion, i.e., the Navier–Stokes equations for incompressible fluids in the Stokes regime, are scarce. Moreover, and whether we use fully fledged CFD numerical models or minimalist singularity solutions, we are always required to deal properly with fluid boundary conditions. All the more so in the Stokes regime, where flows are long-ranged and, hence, boundary effects are all-important. That is particularly relevant for internal fluid dynamics within confined geometries such as the case of cilia driven flows in the KV during zebrafish development.

In recent years, our understanding of the biophysics of left–right symmetry breaking in vertebrates has gain much from minimal approaches [7,12,15,19]. Following a similar strategy, here we have started putting together a minimal biophysical model which reduce the observed vortical fluid flow within in the KV to a set of singular solutions satisfying the imposed boundary conditions; one that is informed by our current understanding of the fluid flow in the KV, that satisfies the requirements for left–right symmetry breaking, but which is also amenable to extensive parametric analysis. Our work is a step forward in this direction. By finding the general conditions for the solution to the fluid mechanics of a singular rotlet within a rigid sphere, we have enlarged the set of available solutions in a way that can be easily extended to more complex configurations.

Author Contributions: I.T. and A.O.G. conceived the research project. Y.H.-P. developed the theory and performed the computations. I.T., A.O.G. and J.M.R.-M. supervised the findings of this work. All authors have read and agreed to the published version of the manuscript.

Funding: Y.H.-P. is a doctoral student from Programa de Doctorado en Ciencias; at the Centro de Investigación en Ciencias, Instituto de Investigación en Ciencias Básicas y Aplicadas of the Universidad Autónoma del Estado de Morelos (UAEM) and received fellowship No. 596195 from CONACYT. In addition, she obtained a research grant from the Ibero-American General Secretariat (SEGIB)-Carolina Foundation-2019. I.T. acknowledges the Spanish

Ministry of Economy and Competitiveness Grant FIS2016-77692-C2-1-P and the Ibero-America Program-Santander Universities 2015.

Acknowledgments: We acknowledge Markus Franziskus Müller at UAEM for fruitful discussions.

Conflicts of Interest: The authors declare no conflict of interest. The funders had no role in the design of the study; in the collection, analyses, or interpretation of data; in the writing of the manuscript, or in the decision to publish the results.

References

1. Gilbert, S.F. *Developmental Biology*, 6th ed.; Sinauer Associates: Sunderland, MA, USA, 2000.
2. Beddington, R.S.P.; Robertson, E.J. Axis development and early asymmetry in mammals. *Cell* **1999**, *96*, 195–209.
3. Hirokawa, N.; Okada, Y.; Tanaka, Y. Fluid dynamic mechanism responsible for breaking the left–right symmetry of the human body: the nodal flow. *Annu. Rev. Fluid Mech.* **2009**, *41*, 53–72.
4. Kartagener, M. Zur Pathogenese der Bronchiektasien. *Lung* **1933**, *84*, 73–85.
5. Afzelius, B.A. A human syndrome caused by immotile cilia. *Science* **1976**, *193*, 317–319.
6. Nonaka, S.; Shiratori, H.; Saijoh, Y.; Hamada, H. Determination of left–right patterning of the mouse embryo by artificial nodal flow. *Nature* **2002**, *418*, 96–99.
7. Cartwright, J.H.E.; Piro, O.; Tuval, I. Fluid-dynamical basis of the embryonic development of left–right asymmetry in vertebrates. *Proc. Natl. Acad. Sci. USA* **2004**, *101*, 7234–7239.
8. McGrath, J.; Somlo, S.; Makova, S.; Tian, X.; Brueckner, M. Two populations of node monocilia initiate left–right asymmetry in the mouse. *Cell* **2003**, *114*, 61–73.
9. Nonaka, S.; Tanaka, Y.; Okada, Y.; Takeda, S.; Harada, A.; Kanai, Y.; Kido, M.; Hirokawa, N. Randomization of left–right asymmetry due to loss of nodal cilia generating leftward flow of extraembryonic fluid in mice lacking KIF3B motor protein. *Cell* **1998**, *95*, 829–837.
10. Okada Y.; Takeda, S.; Tanaka, Y.; Belmonte, J.C.I.; Hirokawa, N. Mechanism of nodal flow: A conserved symmetry breaking event in left–right axis determination. *Cell* **2005**, *121*, 633–644.
11. Nonaka, S.; Yoshiba, S.; Watanabe, D.; Ikeuchi, S.; Goto, T.; Marshall, W.F.; Hamada, H. De novo formation of left–right asymmetry by posterior tilt of nodal cilia. *PLoS Biol.* **2005**, *3*, 1467–1472.
12. Cartwright, J.H.E.; Piro, N.; Piro, O.; Tuval, I. Embryonic nodal flow and the dynamics of nodal vesicular parcels. *J. R. Soc. Interface* **2007**, *4*, 49–55.
13. Kramer-Zucker, A.G.; Olale, F.; Haycraft, C.J.; Yoder, B.K.; Schier, A.F.; Drummond, I.A. Cilia-driven fluid flow in the zebrafish pronephros, brain and Kupffer's vesicle is required for normal organogenesis. *Development* **2005**, *132*, 1907–1921.
14. Supatto, W.; Vermot, J. From cilia hydrodynamics to zebrafish embryonic development. *Curr. Top. Dev. Biol.* **2011**, *95*, doi:10.1016/B978-0-12-385065-2.00002-5.
15. Smith A.A.; Johnson T.D.; Smith D.J.; Blake J.R. Symmetry breaking cilia-driven flow in the zebrafish embryo. *J. Fluid Mech.* **2012**, *705*, 26–45.
16. Ferreira, R.R.; Vilfan, A.; Jülicher, F.; Supatto, W.; Vermot, J. Physical limits of flow sensing in the left–right organizer. *eLife* **2017**, *6*, e25078.
17. Supatto, W.; Fraser, S.E.; Vermot, J. An all-optical approach for probing microscopic flows in living embryos. *Biophys. J.* **2008**, *95*, 29–31.
18. Sampaio, P.; Ferreira, R.R.; Guerrero, A.; Pintado, P.; Tavares, B.; Amaro, J.; Smith, A.A.; Montenegro-Johnson, T.D.; Smith, D.J.; Lopes, S.S. Left-right organizer flow dynamics: How much cilia activity reliably yields laterality? *Dev Cell.* **2014**, *29*, 716–728.
19. Montenegro-Johnson, T.D.; Baker, D.I.; Smith, D.J.; Lopes, S.S. Three-dimensional flow in Kupffer's Vesicle. *J. Math. Biol.* **2016**, *1*, 1432–1416.
20. *Microhydrodynamics: Principles and Selected Applications*; Kim, S., Karilla, S.J.; Eds.; Dover Publications: Mineola, NY, USA, 2005.
21. *Boundary Integral and Singularity Methods for Linearized Viscous Flow*; Pozrikidis, C., Ed.; Cambridge University Press: Cambridge, UK, 1992.
22. Lorentz, H.A. A general theorem concerning the motion of a viscous fluid and a few consequences derived from it. *Versl. Kon. Akad. Wet. Amst.* **1897**, *5*, 168–175.

23. Oseen, C.W. Neuere Methoden und Ergebnisse in der Hydrodynamik. *Leipzig Akad. Verlagsgesellschaft* **1927**, doi:10.1002/zamm.19280080412.
24. Burgers, J.M. On the motion of small particles of elongated form suspended in a viscous liquid. Chap. I11 of Second Report on Viscosity and Plasticity. *Kon. Ned. Akad. Wet. Verhand.* **1897**, *16*, 113–184.
25. Batchelor, G.K. The stress system in a suspension of force-free particles. *J. Fluid Mech.* **1970**, *41*, 545–570.
26. Hancock, G.J. The self-propulsion of microscopic organisms through Iiquids. *Proc. R. Soc. A* **1953**, *217*, 96–121.
27. Broersma, S. Viscous force constant for a dosed cylinder. *J. Chem. Phys.* **1960**, *32*, 1632–1635.
28. Tuck, E.O. Some methods for flows past blunt slender bodies. *J. Fluid Mech.* **1964**, *18*, 619–635.
29. Tuck, E.O. Toward the calculation and minimization of Stokes drag on bodies of arbitrary shape. In Proceedings of the 3rd Australasian Conference on Hydraulics and Fluid Mechanics, Sydney, Australia, 25–29 November 1968; p. 2S32.
30. Taylor, G.I. Motion of axisymmetric bodies in viscous fluids. In *Problems of Hydrodynamics and Continuum Mechanics*; SIAM Publications: Philadelphia, PA, USA, 1969; pp. 718–724.
31. Batchelor, G.K. Slender-body theory for particles of arbitrary cross-section in Stokes flow. *J. Fluid Mech.* **1970**, *44*, 419–440.
32. Tillett, J.P.K. Axial and transverse Stokes flow past slender axisymmetric bodies. *J. Fluid Mech.* **1970**, *44*, 401–417.
33. Cox, R.G. The motion of long slender bodies in a viscous fluid. Part 1. General theory. *J. Fluid Mech.* **1970**, *44*, 791–810.
34. Cox, R.G. The motion of long slender bodies in a viscous fluid. Part 2. Shear flow. *J. Fluid Mech.* **1971**, *45*, 625–657.
35. Blake, J.R.; Chwang, A.T. Fundamental singularities of viscous flow. Part I. The image system in the vicinity of a stationary no-slip boundary. *J. Eng. Math.* **1974**, *8*, 23–29.
36. Hackborn, W.; O'Neill M.E.; Ranger K.B. The structure of an asymmetric Stokes flow. *Q. J. Mech. Appl. Math.* **1986**, *39*, 1–14.
37. Ranger, K.B. The Stokes drag for asymmetric flow past a spherical cap. *J. Appl. Math. Phys.* **1973**, *24*, 801–809.
38. Purcell, E.M. Life at low Reynolds number. *Am. J. Phys.* **1977**, *45*, 3–11.
39. Blake, J.R.; Otto, S.R. Filter Feeding, Chaotic Filtration, and a Blinking Stokeslet. *Theor. Comput. Fluid Dyn.* **1998**, *10*, 23–36.
40. Cartwright, J.H.E.; Piro, O.; Tuval, I. Fluid dynamics in developmental biology: Moving fluids that shape ontogeny. *HFSP J.* **2009**, *3*, 77–93.
41. Boutin, C.; Labedan, P.; Dimidschstein, J.; Richard, F.; Cremer, H.; Andre, P.; Yang, Y.; Montcouquiol, M.; Goffinet, A.M.; Tissir, F. A dual role for planar cell polarity genes in ciliated cells. *Proc. Natl. Acad. Sci. USA* **2014**, *111*, E3129–E3138.
42. Woodhouse, F.G.; Goldstein, R.E. Cytoplasmic streaming in plant cells emerges naturally by microfilament self-organization. *Proc. Natl. Acad. Sci. USA* **2013**, *110*, 14132–14137.
43. Dumortier, J.G.; Le Verge-Serandour, M.; Tortorelli, A.F.; Mielke, A.; de Plater, L.; Turlier, H.; Maitre, J.L. Hydraulic fracturing and active coarsening position the lumen of the mouse blastocyst. *Science* **2019**, *365*, 465–468.